Effect of beryllium filter purity on x-ray emission measurements

2014 Plasma Phys. Control. Fusion 56 125018

(http://iopscience.iop.org/0741-3335/56/12/125018)

IOP Publishing Plasma Physics and Controlled Fusion

Plasma Phys. Control. Fusion **56** (2014) 125018 (6pp) doi:10.1088/0741-3335/56/12/125018

Effect of beryllium filter purity on x-ray emission measurements

M B McGarry[1], P Franz[2], D J Den Hartog[1] and J A Goetz[1]

[1] Department of Physics, University of Wisconsin—Madison, Madison, WI 53706, USA
[2] Consorzio RFX (CNR, ENEA, INFN, Università di Padova, Acciaierie Venete SpA), Corso Stati Uniti 4, 35127 Padova, Italy

E-mail: mbmcgarry@wisc.edu

Received 2 September 2014, revised 21 October 2014
Accepted for publication 31 October 2014
Published 18 November 2014

Abstract

Beryllium foils of the purity grade typically specified for use as filters in soft x-ray (SXR) diagnostics may contain sufficient heavy element impurities to distort the energy transmission response of the filter. Electron microprobe analysis of the foils used in the Madison Symmetric Torus (MST) SXR tomography diagnostic revealed an impurity content of ∼0.3% fractional abundance by weight, comprised primarily of iron, zirconium, chromium, and nickel. These impurities lower the peak filter transmission in the energy range of the detector and alter the shape of the transmission curve. As a result, foil impurities introduce errors in any general measurement where radiation is being filtered. For example, neglecting the effect of impurities on filter transmission leads to large systematic errors (50%) in the electron temperature measured using the SXR double-filter technique on MST.

Keywords: x-ray emission, MST, double-filter, beryllium, impurities

(Some figures may appear in colour only in the online journal)

1. Introduction

Soft x-ray (SXR) emission provides information about magnetic field structure, electron temperature, and impurity content in experimental plasmas [1–6]. Beryllium is used as an x-ray filter due to its smooth x-ray transmission curve, and research-grade foils commonly used for this application have manufacturer-stated purities of 99.8–99.9% . This paper presents the results of an investigation to quantify the nature and impact of impurities in such a foil, purchased from a major commercial supplier of research-grade high-purity beryllium foils. These foils have a specified total purity, and are certified with upper limits on specific elements. If heavy element impurities are present, even at relatively small concentrations of ∼0.1% fractional abundance by weight, they will significantly impact absolute SXR brightness measurements. These impurity levels also lead to systematic errors greater than 10% in electron temperature (T_e) measurement using the double-filter technique. However, if the impurity content can be accurately catalogued, then an effective transmission curve can be modeled, leading to a good agreement between the simulated SXR brightnesses and measurements.

This paper is organized as follows: section 2 describes the experimental setup of the SXR diagnostic at the Madison Symmetric Torus (MST) and shows the geometry of the detectors that provide brightness profile measurements. Section 3 reports the quantitative impurity concentration measurements that were performed on the foils after the brightness measurement variation was identified. Section 4 highlights the impact of these impurity concentration levels on the overall transmission functions of the detectors, as well as on the resulting x-ray emissivity and electron temperature measurements.

2. Experimental setup

2.1. Diagnostic description

On MST, a reversed field pinch magnetic confinement device, a SXR diagnostic measures line-integrated brightness profiles at multiple poloidal angles in two distinct energy bands [7, 8]. These measurements are tomographically reconstructed into a poloidal emissivity map. Additionally, the paired measurements through different beryllium filters are compared to determine electron temperature (T_e) using the double-filter technique [9].

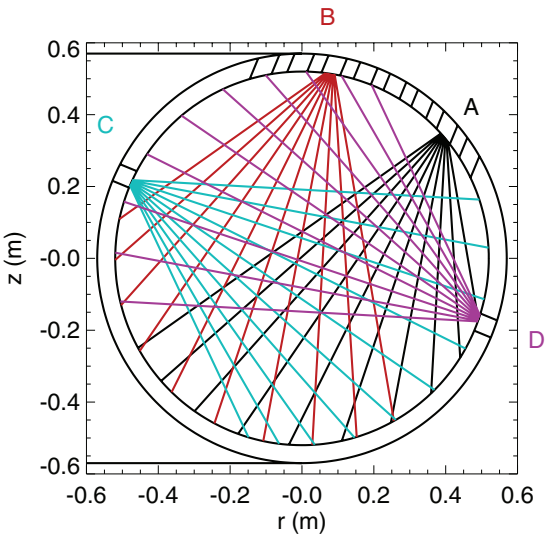

Figure 1. Geometry of the MST SXR double-filter diagnostic. Four detectors each with 10 unique chords at a single poloidal location have intersecting lines-of-sight to enable tomographic reconstruction. Each chord is comprised of two photodiodes separated toroidally and filtered with different beryllium foil thicknesses for T_e measurement.

The SXR diagnostic on MST is comprised of four separate detectors separated poloidally at a single toroidal location. Each detector has two columns of 10 silicon photodiodes, providing a total of 40 unique lines-of-sight. Each column of diodes has its own filter and pinhole, and the cones-of-sight for the two columns (with a small toroidal separation) overlap in the plasma. As a result, each pair of diodes can be considered as viewing the same plasma volume, one through a thin filter and the other through a filter approximately twice as thick. One column has a 421 μm beryllium filter, while the other column has an 857 μm filter. Two diodes looking at the same plasma through different filters sample different components of the energy distribution, so their measured brightness is used to calculate electron temperature. Figure 1 shows the overlapping lines of sight for the four detectors, providing two nominally horizontal profiles (A, B) and two nominally vertical profiles (C, D). The layout of the detectors at 90 degree intervals also allows for two simultaneous tomographic reconstructions of SXR emissivity, one for each filter thickness.

The ratio of the two brightnesses approximately gives the hottest T_e along the line-of-sight, via the double-foil technique [10, 11]. In practice, the relationship between the ratio of brightnesses (R) and plasma temperature is determined by generating a library of T_e versus R curves using a model of SXR emission [12]. The model calculates x-ray emission assuming a pure bremsstrahlung SXR spectrum and uses T_e and n_e profiles as a function of radius (r) that are well described using an alpha-model:

$$T_e(r) = T_e(0)\,(1 - (r/a)^{\alpha})^{\beta} \tag{1}$$

where $T_e(0)$ is the temperature at the core and a is the minor radius of the MST device. The canonical n_e and T_e profiles on MST are axisymmetric and monotonically decreasing, with $\alpha \sim 8$ and $\beta \sim 8$ [13]. Because the double-foil technique is relative, continuum contributions such as Z_{eff} or recombination radiation, can be ignored.

The $T_e(R)$ library is then made by generating synthetic emissivities for different plasma temperatures, and calculating the expected line-integrated brightness signal at each detector by incorporating the detector geometries and the transmission and absorption functions for the beryllium filters and the silicon photodiodes. Finally, the ratio of the signals through the thin to thick filter is calculated for each possible T_e, and a curve is generated for the full range of possible temperatures.

The transmission and absorption functions for the detector response are modeled using photo-absorption coefficients from the Lawrence Berkeley National Laboratory Center for x-ray Optics (CXRO) database[3]. For the cases presented below where the beryllium is not pure, the effective transmission curve of the filter has been calculated by defining an effective mass absorption coefficient (μ_{eff}). For example, the transmission function (T) for a foil comprised of beryllium and zirconium can be modeled as:

$$T = e^{-\rho d \mu_{eff}} \tag{2}$$

$$\mu_{eff} = \frac{x\mu_{Be}A_r^{Be} + y\mu_{Zr}A_r^{Zr}}{xA_r^{Be} + yA_r^{Zr}} \tag{3}$$

where ρ is average density of the material in gm cm^{-3} and d is the thickness in cm. The equation for μ is easily expanded for multiple impurity species: x and y are the fractional abundance by weight of beryllium and zirconium, and A_r is the atomic weight of the element.

2.2. Effect of foil impurities on measured brightness

A mixed foil configuration including beryllium foils from two separate material lots, installed on MST in December 2012 (after the publication of [9]), resulted in systematic differences in the brightness measured from different poloidal angles, despite nominally identical detectors and electronics. All the detectors use stacks of ~80 μm beryllium foils to achieve identical total filter thickness. The thicknesses of the individual foils have been carefully measured using a high-precision micrometer with an uncertainty of ± 1 μm. Figure 2 compares the brightness profiles from the four detectors in the 421 μm thin energy band (top) and 857 μm thick energy band (bottom), as a function of impact parameter (shortest distance between the chord and the geometric center of MST). Within a given filter thickness, all four probes should measure approximately the same brightness at an impact parameter of 0.0 m for an axisymmetric emission profile. This is nominally true for the thick filter measurements, where probe variation is due to lower signal-to-noise. The thin filter measurements, on the other hand, show a systematic increase in signal of 10–15% for two of the profiles (diamonds) compared with the other two profiles (dots).

The beryllium foils for the four thick filter detectors (857 μm) are all from a single batch of beryllium that was described by the manufacturer as being 99.8% pure beryllium. The 421 μm filters for detectors C and D were also comprised

[3] http://henke.lbl.gov/optical_constants/ accessed 26 August 2014.

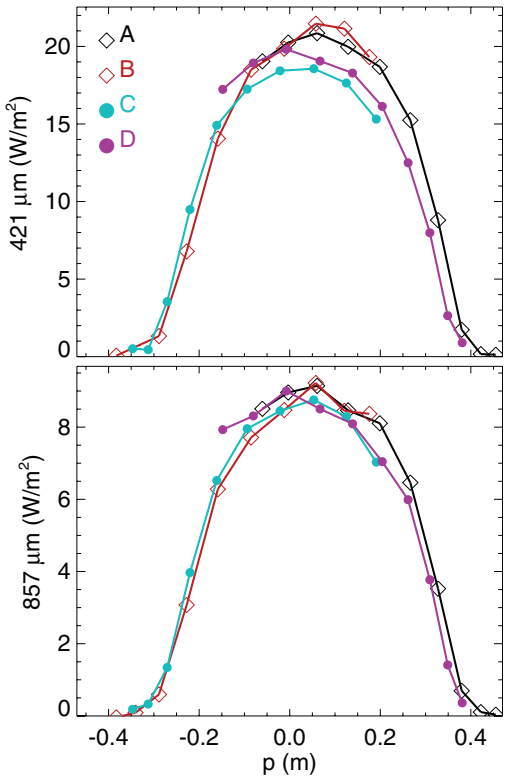

Figure 2. Measured SXR brightness profiles for the four detectors as a function of impact parameter through a 421 μm filter (top) and 857 μm filter (bottom). The thin filter plot illustrates a significant difference in amplitude, greater than 10%, between profiles A and B (diamonds) compared with C and D (dots) due to different impurity content in the filters. The thick filter measurements all have identical foil purity, and the differences between these profiles are primarily due to systematic differences in the detector geometries, as well as some electronic noise.

entirely from the 99.8% pure beryllium. The 421 μm filters for detectors A and B were predominantly the 99.8% pure beryllium, but included 88 and 92 μm, respectively, of 99.9% pure beryllium from a different material lot purchased from the same company. Inspection of the company-provided material data sheet for the two batches indicated that the 99.8% pure beryllium also contains an additional 0.1% contribution from zirconium, 99.9% pure beryllium batch does not contain significant levels of zirconium or other heavy elements. The amplifiers, and digitization electronics are identical across detectors. The geometric properties of the four detectors were also carefully checked in the design drawings and verified after fabrication. The silicon photodiodes have varying effective thickness across the profiles, but this effect is less than 2% and affects both thin and thick filters equally [14, 15]. It was then clear that the differencies in the brightness profiles measured from the different probes could be attributed to impurities in the foils.

3. Quantitative impurity measurements using microprobe analysis

After identifying that the impurity content of the two batches of foil was not identical, spectral analysis was done on a sample from each batch to quantify the impurity content, using an electron microprobe. The microanalysis was performed by wavelength dispersive electron probe microanalysis (EPMA) with a CAMECA SX51 at the University of Wisconsin-Madison Department of Geoscience. EPMA is a rigorous quantitative technique that utilizes an electron beam to ionize target atoms and produce characteristic x-rays [16]. The analytical volume is ~1 cubic micron for materials of atomic number 12–15 and an accelerating voltage of 15 keV. It varies directly with beam voltage and inversely with increasing atomic number.

This analysis looked at elements that could distort the transmission function between 2–8 keV and had been tested for in the commercial analysis. Seven elements (Se, Zr, Cr, U, Ca, W and Fe) were considered, using the TAP, PET and LIF diffracting crystals of the SX51 [17]. Measurements on the two foils (45, 94 um) and standards were performed at 10, 15, and 20 keV beam energies, and processed using the STRATAGem software program[4]. Table 1 shows the values reported by the manufacturer and the microprobe results of the elements found to be detectable using the 20 keV beam, which is representative of the bulk material, for both the 99.9% and 99.8% pure foils. Se, U, Ca and W were tested for but measured as non-detect. The impurity concentrations are calculated by averaging twenty spatially separated measurements on a single foil sample, and are listed in fractional abundance by weight. The relative standard deviation (RSD) provides an estimate of the range of the 20 measurements.

The measured values of zirconium were consistent with the information provided by the company and indicate that zirconium is a substantial impurity at 0.1% of the total mass of the lower-purity foil, while there was no detectable zirconium in the higher purity foil. More surprisingly, both foils show higher than expected levels of iron, nickel, and chromium, indicating stainless steel contamination. Although traditional EPMA is a bulk technique, thin films can also be measured by acquiring x-ray intensities on both the film and bulk standard at several different accelerating voltages and then applying special software which uses a physical x-ray generation/absorption depth profile model to back out a consistent thin film composition [18]. An additional scan was done at 25 keV, where there is effectively no ionization in a thin film, which confirmed that the stainless steel is present in the bulk material and is not simply a surface film deposited during fabrication.

Most concerning is that the lower-purity foil has an average iron content of 0.354%, which is an order of magnitude larger than expected, and outpaces the increases due to stainless steel alone. The impurities also have high RSD, indicating that there was large spatial variation of the measurements. For homogeneous materials, RSD is typically a few percent, so it can be concluded that these impurities are salted through the material in relatively large clumps. In fact, the distribution of the iron measurements is highly asymmetric, with a mode around 0.2% and a tail toward higher impurity content. Combining the iron and zirconium measurements in the lower-purity foil easily reduces the overall beryllium purity to below 99.7%.

[4] www.samx.com accessed 26 August 2014.

Table 1. Impurity content as quoted by the manufacturer versus the value measured by electron microprobe analysis, in fractional abundance by weight, for the two batches of beryllium. 25 keV microprobe beam energy ensures measurements are bulk. Relative standard deviation (RSD) provides an estimate of the range of measurements in the set of 20 spatially unique measurements from a single foil.

	'99.9%' Be			'99.8%' Be		
Element	Manufacturer	Microprobe	RSD	Manufactuer	Microprobe	RSD
Cr	0.0005	0.0040	90%	0.001	0.070	87%
Fe	0.010	0.065	40%	0.0175	0.354	73%
Ni	0.020	0.017	27%	0.0085	0.0230	74%
Zr	0.00	Non-detect	—	0.1025	0.1000	49%

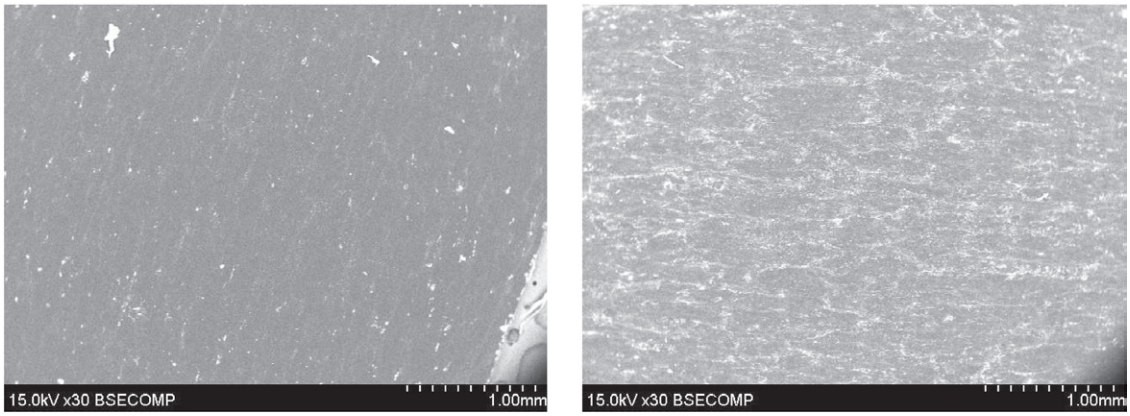

Figure 3. BSE image of bulk structure for the high-purity foil (left), and the lower-purity foil (right), using a 15 keV beam and 30x magnification. Bright regions of impurities are much more prevalent in the lower-purity foil and exhibit granular boundary structure.

Backscatter electron (BSE) imaging of the two samples confirmed the granular nature of the impurity distribution. Figure 3 shows the structure of the bulk region at 30x magnification (using a 15 keV beam) for the higher purity sample (left) compared with the lower purity sample (right). Bright regions in the image were confirmed with targeted spectral analysis to be impurities, predominantly iron, chromium, nickel, and zirconium. Notably, the lower-purity foil shows significant impurity structure, likely representing granular boundaries.

4. Impact of impurities on SXR measurements

4.1. Line integrated brightness

Heavy element impurities at levels of ~0.1% can significantly alter the transmission function of beryllium in the SXR energy range. A new transmission curve was calculated to accurately reflect the impurities present in the beryllium filters used on MST. Figure 4 (top pane) shows the transmission function for a 421 μm pure beryllium filter (red dashed) compared with the transmission function for a filter including the measured impurities for the lower-purity foil listed in table 1 (black solid), with uncertainty in the theoretical value of μ denoted as blue shading. The bottom pane folds in the photodiode response to show the overall measurement sensitivity versus energy assuming an ideal beryllium versus an impure beryllium filter. The addition of a total of 0.3% impurities in the filter has a dramatic effect on total detector response, as well as shifting the peak response toward higher energy.

The theoretical transmission function shown in figure 4 has been applied to the data presented in section 2.2. Properly accounting for the mixed pure and contaminated beryllium foils in SXR-A and SXR-B leads to a theoretical brightness 16% larger than the signals for SXR-C and D (which had only contaminated foils). This 16% correction has been applied to the brightness profiles from figure 2, resulting in agreement to within 5% across the four profiles, which is within experimental uncertainties.

4.2. T_e measurement

Although measurement of T_e from SXR brightness is a relative measurement, it can also be impacted by the presence of impurities in the filter because the shape of the overall transmission function is changed. Figure 5 illustrates the danger in assuming a pure beryllium filter when using the double-filter technique to determine T_e. The SXR model described in section 2 is used to simulate the bremsstrahlung emissivity of a 1.5 keV plasma. The simulated emissivity is then integrated along the detector lines-of-sight and convolved with the detector sensitivity and filter transmission functions, which include the filter impurities, to generate a synthetic dataset for the brightness recorded through both thin and thick filters. The $T_e(R)$ libraries are used to apply the double-filter technique to the synthetic brightnesses and calculate expected T_e as a function of impact parameter (p). The black diamonds represent the temperature calculated using a model $T_e(R)$ library that also includes the filter impurities, and yields the anticipated

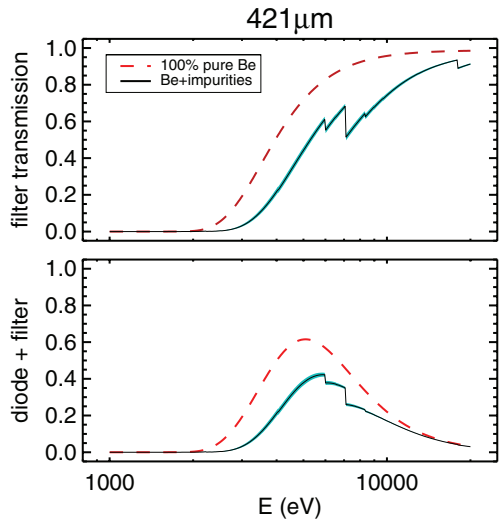

Figure 4. Theoretical filter transmission functions for a 421 μm pure beryllium filter (red dashed) and for a filter containing heavy element impurities as listed in table 1 (top). A 5% uncertainty in μ is denoted by blue shading. The overall sensitivity curve including both the filters and the photodiode response is plotted in the bottom pane. Although the total impurity content is only ∼0.3%, the detector response is dramatically impacted.

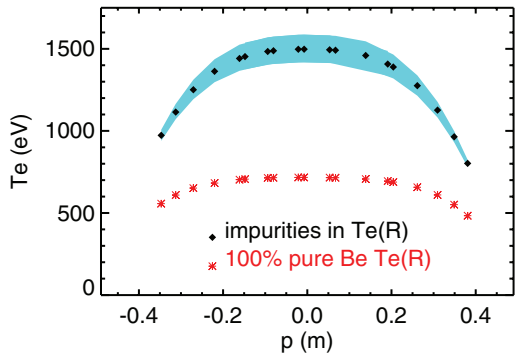

Figure 5. Double-filter T_e is calculated from a synthetic data set that incorporates the effect of filter impurities on the recorded signal. Diamonds show that if the impurities are also included in the modeled $T_e(R)$ ratio library then the expected core T_e of 1500 eV is recovered. If however, the $T_e(R)$ library assumes pure beryllium filters, then the calculated temperature is dramatically underpredicted (stars). Blue shading represents the variation in T_e due to uncertainty in the value of μ_{eff} given by CXRO.

core T_e of approximately 1.5 keV. In contrast, the red stars represent a synthetic dataset that properly includes the impurity content of the filters but then applies a $T_e(R)$ library that is based on pure beryllium. When the pure beryllium $T_e(R)$ library is used, the estimated T_e is much lower than the true value of 1.5 keV. This plot makes clear that it is critical to have an accurate assessment of filter purity.

An additional source of uncertainty in this technique is associated with the theoretical photoabsorption coefficients themselves. A simulation of the coefficients with the maximum stated uncertainty of 5% [19] leads to a 6% change in T_e, as seen in the blue shading. Because this is a non-trivial source of systematic error, we plan to experimentally verify the transmission function for the filters in the 1–10 keV energy range. After verification, we will apply the new transmission functions to the double-filter temperature calculation and compare the resulting temperature with our Thomson scattering diagnostic to benchmark the technique.

5. Summary and conclusions

Nominally pure beryllium foils are used as energy filters for the SXR tomography and T_e diagnostic on the Madison Symmetric Torus. A mix of filters from two different manufacturing batches was found to have different transmission curves, although both batches were at least 99.7% pure beryllium. Commercially fabricated beryllium foils are typically ∼99.8% stated purity, and have historically been considered sufficiently pure for use in plasma physics experiments. However, this paper demonstrates that heavy metals can distort the x-ray transmission properties of the filters, even at low concentrations.

An impurity content of ∼0.3%, comprised predominantly of heavy metals, has been characterized using an electron microprobe. Composite material analysis has quantified the relative contributions of iron, zirconium, chromium and nickel, which distort the overall transmission function of the filter. This distortion impacts both the peak transmission and also the shape of the curve. As a result, absolute amplitude of the measured brightness as well as the T_e determined through the double-filter technique are compromised. The impurities have been added to filter transmission model, and the SXR brightness calculation has been corrected. $T_e(R)$ curves including the impurity content of the filters can be found and applied to the measurements. However, before any calculation and comparison with other T_e data (like the one from Thomson Scattering) is made, the Te from SXR needs accurate transmission functions of the foils from direct measurements in the range 1–10 keV.

Experimenters should carefully assess the purity of their beryllium foils and actively check for heavier elements that may block transmission in the energy range of interest. If present, impurities can be quantified and folded into a transmission model by calculating the effective mass absorption coefficient of the composite material.

Acknowledgments

The authors would like to thank J Fournelle at the University of Wisconsin-Madison Department of Geoscience and John Jacobs at the University of Wisconsin-Madison Material Science Center for their materials analysis contributions. E Gullikson and J Johnson also provided valuable insight and experience. This material is based upon work supported by the US Department of Energy, Office of Science, Office of Fusion Energy Sciences under Award Number DE-FC02-05ER54814.

References

[1] Granetz R S and Camacho J F 1985 *Nucl. Fusion* **25** 727
[2] Kiraly J *et al* 1987 *Nucl. Fusion* **27** 397

[3] Granetz R S and Smeulders P 1988 *Nucl. Fusion* **28** 457
[4] Navarro A P, Ochando M A and Weller A 1991 *IEEE Trans. Plasma Sci.* **19** 569
[5] Delgado-Aparicio L *et al* 2013 *Phys. Rev. Lett.* **110** 065006
[6] Franz P, Gobbin M, Marrelli L, Ruzzon A, Bonomo F, Fassina A, Martines E and Spizzo G 2013 *Nucl. Fusion* **53** 053011
[7] Dexter R N *et al* 1990 *Fusion Techonol.* **19** 131
[8] McGarry M B, Franz P, Den Hartog D J and Goetz J A 2010 *Rev. Sci. Instrum.* **81** 10E516
[9] McGarry M B, Franz P, Den Hartog D J, Goetz J A, Thomas M A, Reyfman M and Kumar S T A 2012 *Rev. Sci. Instrum.* **83** 10E129
[10] Jahoda F C, Little E M, Quinn W E, Sawyer G A and Stratton T F 1960 *Phys. Rev.* **119** 843
[11] Donaldson T P 1978 *Plasma Phys.* **20** 1279
[12] Bonomo F, Alfier A, Gobbin M, Auriemma F, Franz P, Marrelli L, Pasqualotto R, Spizzo G and Terranova D 2009 *Nucl. Fusion* **49** 045011
[13] Reusch L M, Galante M E, Franz P, Johnson J R, McGarry M B, Stephens H D and Den Hartog D J 2014 *Rev. Sci. Instrum.* **85** 11D844
[14] Franz P, McGarry M B, Den Hartog D J, Goetz J A and Johnson J 2014 *41st EPS Conf. on Plasma Physics Proc.* (*Berlin, Germany*, *23–7 June 2014*)
[15] McGarry M B, Franz P, Den D J, Goetz J A and Johnson J 2014 Effect of photodiode aluminum cathode frame on spectral sensitivity in the soft x-ray energy band *Rev. Sci. Instrum.* **85** 096105
[16] Reed S J B 1993 *Electron Microprobe Analysis* 2nd edn (Cambridge: Cambridge University Press) p 326
[17] Donovan J, Kremser D, Fournelle J and Goemann K 2014 *Probe for EMPA v. 10.3.5: User's Guide and Reference* (Eugene, OR: Probe Software, Inc) p 414 (probesoftware.com/Technical.html)
[18] Pouchou J-L 2002 *Mikrochim. Acta* **38** 133
[19] Gullikson E 2014 private communication with M B McGarry